Data Supplements

Computational Methods - Crystallographic coordinates for paclitaxel complexed with αβ-tubulin (1JFF) were obtained from the PDB (1). A complementary model which proposed the T-Taxol structure (2) has been successfully used for the prediction of novel PTX analogs (3). Hydrogen atoms and lone electron pairs were added, and all atoms were typed for the Weiner/Kollman (4) (implemented as "Kollman All Atom" in Sybyl 7.0; Tripos, St. Louis, MO) and the Cornell/Kollman (5) ("Amber94" in MOE 2004.03; Chemical Computing Group, Montreal, Canada) force fields. All residues were minimized to shallow local minima (5 kcal gradient) in order to reduce the overall FF energy, but remain close to the crystallographically defined coordinates. Due to a lack of Kollman force field parameters for MAC-321's furan moiety, subsequent computational comparisons were limited to the two analogs with phenyl substitution at C3', paclitaxel, and docetaxel. Additional calculations performed using the more general Tripos force field suggest that MAC-321 behaves very similar to docetaxel. As a result we take docetaxel as a structural surrogate for MAC-321 consistent with their similar activities. The tubulin-docetaxel complex was derived by structurally modifying the 1JFF PTX-tubulin complex followed by optimization of the new ligand within the rigid receptor in preparation for the next layer of calculations.

The ligands plus all atoms of residues within a 5.0 Å radius of PTX and docetaxel in the wild type tubulin models (Asp at position 26) were then freely optimized to convergence with a gradient cutoff of 0.5 kcal using the Amber94 force field in MOE, dictionary charges, and a Poisson-Boltzman (PB) reaction field solvation model. The latter employed an exterior dielectric constant of 80.0 and an interior dielectric constant of 1.0 (http://www.chemcomp.com/Journal_of_CCG/Features/pboltz.htm). The remaining atoms of the

tubulin dimer were tethered to their original positions with a 1000 kcal force constant. Both wild type systems converge rapidly with little positional variance relative to the starting coordinates (refer to Fig. 7A).

The Asp26 residues in the PTX and docetaxel minimized complexes were mutated to Glu. All possible rotamers of the Glu side chain were analyzed for their respective interaction potentials within each complex using both the Lovell rotamer database (6) implemented in Sybyl and systematic bond-by-bond rotation in MOE. Each approach identified the same two residue positions as most favored (R1 and R2, Fig. 7b, Table 1S). The library-driven analysis using the Lovell rotamer database revealed that the most abundant of eight possible conformers (χ_1 -67°, χ_2 180°, χ_3 -10°) was unavailable to any of the ligands (i.e. paclitaxel, docetaxel and MAC-321) as a result of severe steric conflicts with the C-3' NHR side chains. "Severe" in this context is defined as contact between surfaces projected at 0.6 times the atomic VDW radii. Only three rotamers corresponding to rotation of the Glu carboxylate around the Cβ–Xγ bond fell within the maximal contact cutoff (Fig. 7b, R1-R3). Similar treatment of the other rotamer complexes reveals that R3, which places the Glu carboxylate deeper into the pocket, produces too great a steric penalty to be viable for either ligand. R1, which directs its carboxylate into solvent, can be sterically accommodated by either ligand, but with loss of the favorable electrostatic and hydrogen-bonding interactions. With the Glu side chain in this orientation, no distinction between ligands is evident.

The systematic method, using a smaller steric interaction parameter (Lovell rotamer testing in Sybyl uses a 0.9 VDW multiplier, while "Rotamer Explorer" in MOE uses a 0.6 VDW multiplier), yielded one additional conformer found at 1% in the rotamer database (R3, Fig. 7b, Table 1S). All three possible starting interactions for the PTX and docetaxel Glu mutants (cf.

Table 1S) were subjected to a further cycle of minimization to give the nearest local minima using identical AMBER 94/PB computational protocols in MOE as described above.

Table 1S. Table of ligand/tubulin interaction statistics

Rotamer	Ligand	ΔG[1] kcal/mol	Strain E[1] kcal/mol	H SA[1] Å^2	HB[1]	chi1	chi2	chi3	Min.
R1	paclitaxel	0.5	0.01	17.4	0	-180	60	0	no
R2	paclitaxel	0.8	0.01	18.0	1	-180	-180	0	no
R3	paclitaxel	1.8	0.3	6.0	2	-180	-70	80	no
R1	docetaxel	0.1	0.01	21.7	0	-180	60	0	no
R2	docetaxel	1.3	0.3	15.7	1	-180	170	0	no
R3	docetaxel	1.7	0.3	10.0	2	-180	-70	80	no

[1]Columns for ΔG, torsional strain, Δ hydrophobic surface area, and hydrogen bonds were calculated in MOE version 2004.03.

The following details of methods used in generating **Table 1S** are quoted from:

http://www.chemcomp.com/Journal_of_CCG/Features/rotexpl.htm

Estimating ΔG. The Rotamer Explorer estimates ΔG, the change in free energy of solvation between two states: protein without side chain (receptor) and side chain each in isolation, and the complex of the two.

For each state, the seven contact types for all contacts between atoms, and between atoms and solvent, are computed. This provides seven descriptors, each one being the *change* in contact surface area between protein and side chain each in isolation, and the complex.

These descriptors were used to model ΔG with a regression fit using a database of small molecules and their solvation energies. Not all of the descriptors are well-represented by the data therein; some coefficients were determined by hand and trial-and-error. The fit (in kcal/mol per square angstrom of weighted surface area) was found to be the sum of the following terms:

- -0.049 hydrogen-bonding/polar
- -0.154 hydrogen-bonding/hydrogen-bonding (favorable)
- -0.052 hydrogen-bonding/hydrogen-bonding (unfavorable)
- +0.004 hydrogen-bonding/hydrophobic

In addition to the change in free energy of solvation, the term for the torsional strain energy of the rotamer discussed above in the *Generation of Rotamers* section was added.

Although the Rotamer Explorer also reports the change in hydrophobic surface area (the integral of hydrophobic character over all exposed surface) and explicit hydrogen bonds, these do not factor into the ΔG scoring function. They are provided for information purposes only.

Strain energy explicitly refers to rotational strain in the rotamer and is taken directly from the Amber94 torsions for the side chain.

Change in exposed hydrophobic surface area (HSA) is calculated relative to glycine in the same position for all rotamers.

Microtubule stability. Examination of the electron crystallographic α,β-tubulin dimer suggests a mechanism by which the Asp26Glu mutation might contribute to microtubule destabilization. The taxane binding site within β-tubulin is located at an interface between the lateral M-loop, the B9-B10 loop, and inner helices H1 and H7 (refer to Fig. 7A in ref (2)). The long H1 and H7 helices of β-tubulin extend from the intradimer interface above the non exchangeable nucleotide binding site of alpha to positions flanking the exchangeable nucleotide site at the growing end (+) of the protofilament. Lengthening of Asp 26, located

on H1, to Glu places the carboxylate group approximately 3Å closer to electrostatically complementary B9-B10 residues such as Arg359. This may result in small allosteric changes that shift the polymeric equilibrium toward disassembly. This is supported by the enhanced activity observed for microtubule destabilizers that bind at the colchicine (B9-B10 region) or vinca (E-site end of H1) sites (Table 1). Binding of stabilizers to the pocket could counter the changes, restoring polymerization potential to near normal levels to produce the observed resistance.

Figure 1S: Sequencing chromatograms of β-tubulin cDNA around codon 26 derived from KB-3-1 parental and KB-15-PTX/099 cell lines. The cDNA derived from β-tubulin mRNA of the indicated cell lines was sequenced using forward and reverse sequencing primers. Nucleotide signals from representative strands are displayed. Note that only the mutant nucleotide is seen in KB-15-PTX/099 β-tubulin sequence. The color code of the nucleotide peaks shown is G(black), A(green), T(red) and C(blue).

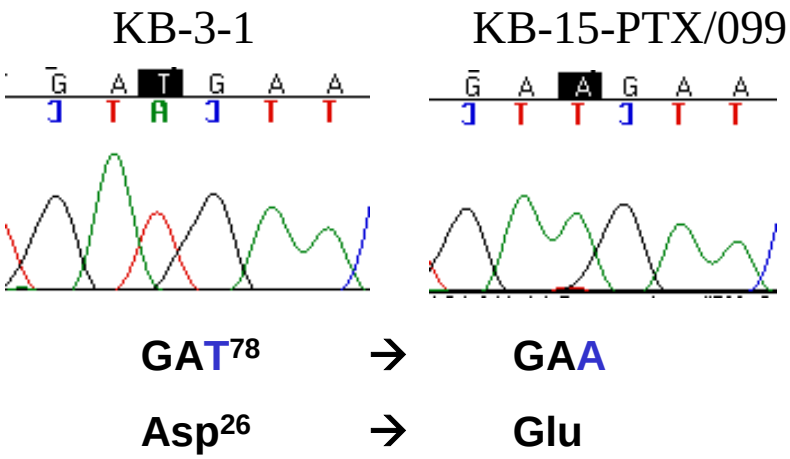

REFERENCES:

1. Lowe J, Li H, Downing KH, Nogales E. Refined structure of alpha beta-tubulin at 3.5 Å resolution. J Mol Biol 2001;313:1045-57.
2. Snyder JP, Nettles JH, Cornett B, Downing KH, Nogales E. The binding conformation of Taxol in beta-tubulin: a model based on electron crystallographic density. Proc Natl Acad Sci U S A 2001;98:5312-6.
3. Ganesh T, Guza RC, Bane S, et al. The bioactive Taxol conformation on beta-tubulin: experimental evidence from highly active constrained analogs. Proc Natl Acad Sci U S A 2004;101:10006-11.
4. Weiner SJ, Kollman PA, Nguyen DT, Case DA. An all atomic force field for simulations of proteins and nucleic acids. J. Comp. Chem. 1986;7:230.
5. Cornell, W.D., Cieplak, P., Bayly, C.I., Gould, I.R., Merz, K.M. Jr., Ferguson, D.M., Spellmeyer, D.C., Fox, T., Caldwell, J.W., Kollman, P.A. A second generation force field for the simulation of proteins and nucleic acids. J. Am. Chem. Soc. 1995; 177: 5179-5197.
6. Lovell SC, Word JM, Richardson JS, Richardson DC. The penultimate rotamer library. Proteins 2000;40:389-408.